Int. J. Heat Mass Transfer. Vol. 20, pp. 647–654. Pergamon Press 1977. Printed in Great Britain

BUBBLE FORMATION AND HEAT TRANSFER DURING DISPERSION OF SUPERHEATED STEAM IN SATURATED WATER—II

HEAT TRANSFER FROM SUPERHEATED STEAM BUBBLES TO SATURATED WATER DURING BUBBLE FORMATION

HANS SCHMIDT
Institut für Reaktorbauelemente, Gesellschaft für Kernforschung, 75-Karlsruhe, Germany

(*Received* 17 *March* 1976 *and in revised form* 12 *August* 1976)

Abstract—In evaporators, which are characterized by introduction of superheated steam into water to be evaporated, the steam is distributed over so-called nozzle plates. The steam is introduced into water through a multitude of cylindrical bores. Regarding the optimum construction of such evaporators, the minimum path of heat transfer is of interest, which is covered by the superheated steam bubbles until reduction of their superheat. On account of its magnitude the energy transport during bubble formation can become significant for the total transport of energy.

In Part I a report was given of the formation of superheated steam bubbles, their size, shape and frequency of formation at high system pressure, and system temperature.

This part of the work describes the heat transfer during the period of bubble formation.

In the range of system pressures considered in the experiment of 15–160 at a decrease in superheat temperature of 40–60% is measured during bubble formation. The average heat-transfer coefficients range from 0.05 to 0.75 W/cm² K. The heat transfer is indicated by a relation of the Stanton number as a function of the Reynolds number.

NOMENCLATURE

b, Laplace constant;
c_p, specific heat;
d, orifice diameter;
g, specific free enthalpy;
h, temperature measuring point;
$\dot{m}$, mass flow rate;
p, pressure;
r, latent heat;
s, enthalpy;
q, heat flux;
V, specific volume;
O, surface;
T, temperature;
Re, $\frac{\dot{m}}{d\eta_0}$, Reynolds number;
Nu, $\frac{\alpha b}{\lambda}$, Nusselt number;
Pe, $\frac{\dot{m}c_p}{\lambda d}$, Péclet number;
St, $\frac{\alpha b d}{\dot{m}c_p}$, Stanton number.

Greek symbols

α, heat-transfer coefficient;
η, viscosity;
λ, thermal conductivity;
Δ, difference;
ν, kinematic viscosity;
ρ, density;
σ, surface tension;
τ, response time.

Indices

Ab, detachment;
O, orifice;
V, antechamber;
$'/''$, saturation state of water/steam phase.

INTRODUCTION

ALTHOUGH the energy or mass transport between bubbles and liquids resemble one another considerably during the period of bubble ascent and bubble formation, the values obtained for bubble ascent can be applied to a limited extent only to non-steady-state processes taking place during bubble formation.

This holds in particular if the resistance to transfer is on the gas side. According to Grassmann [1] the velocity at which the gas enters the liquid via the orifice is mostly much higher than the velocity of bubble ascent. During the process of formation the content of the bubble is very thoroughly mixed up due to the supply of steam through the orifice so that mostly more than half of the initial thermal unequilibrium decays during bubble formation.

L'Ecuyer [2] quotes measurements by which the transition from steam into dry nitrogen bubbles was determined during bubble formation. According to these measurements the detaching bubble was saturated by steam up to 40 and 65% while an increase in mass transfer was achieved by enhancement of the liquid vapor pressure. Conversion of these values on the assumption that an analogy exists between the heat and mass transfer gives heat-transfer coefficients $\alpha = 0.015$–0.03 W/cm² K. Experiments with nitrogen and water and ethyl alcohol, respectively, were per-

formed by L'Ecuyer [2]. Nitrogen was injected through orifices of 1.6 and 0.8 mm diameter. The temperature difference between the heated liquid and the precooled nitrogen was approximately 155 K. For a mass flow of 2.25×10^{-3} to 12.7×10^{-3} g/s changes of temperature of the injected gas during the period of bubble formation was observed to be 55–90% of the overall temperature difference. The heat-transfer coefficient ranged from 0.01 to 0.02 W/cm^2 K. In these experiments the heat and mass transport, respectively, moves from the liquid into the gaseous phase.

Grassmann and Wyss [3] reported upon experiments performed in water with steam entering in a superheated state. The superheat of steam flows towards the interface and a so-called heat-transfer coefficient on the steam side was derived from it. Integral heat-transfer coefficients were indicated in the range of 0.012–0.08 W/cm^2 K, i.e. values averaged over bubble formation and ascent. A strong dependence was observed of the heat-transfer coefficients on the steam inlet temperature and the liquid temperature. To provide an explanation for the observed increase in the α-values with increasing liquid subcooling, they used a model of a boundary layer which is laminar on the steam side and has a given thickness. The steam hitting the phase boundary condenses due to its own low thermal energy and due to the water subcooling. This implies that the steam boundary layer is sucked off which is thus reduced with increasing subcooling. In the reverse case where water evaporates into the bubble, it is assumed that the molecules entering the steam phase will entail an increase in the boundary layer and consequently a decrease in heat transfer.

A summarizing representation of bubble formation at orifices with heat and/or mass transfer taking place simultaneously has not yet been achieved. This is probably due to the multitude of individual observations required from the fact that the physical parameters are multiple and that measuring problems are encountered in two-phase states.

EXPERIMENTAL SETUP AND MEASURING EQUIPMENT

This work is an experimental study of heat transfer from superheated steam to water during bubble formation at single orifices as a function of the system pressure.

The following variables are necessary to provide information about heat transfer:

The mass flow rate through the orifice, the area of exchange surfaces, the temperature differences between the steam and the water at different levels, and the system pressure. The test setup, the determination of the size and shape of the interface, and of the frequency of bubble formation have been described in Part I.

The experiments have been so performed that the superheated steam has been introduced into saturated water. The value of the system pressure is sufficient to determine the state of water. The requirement that the temperature difference between the steam and the water phases must be measured without influencing the interface and the kinetics of the system resulted in the development of a new needle-shaped thermocouple (Fig. 1) [4].

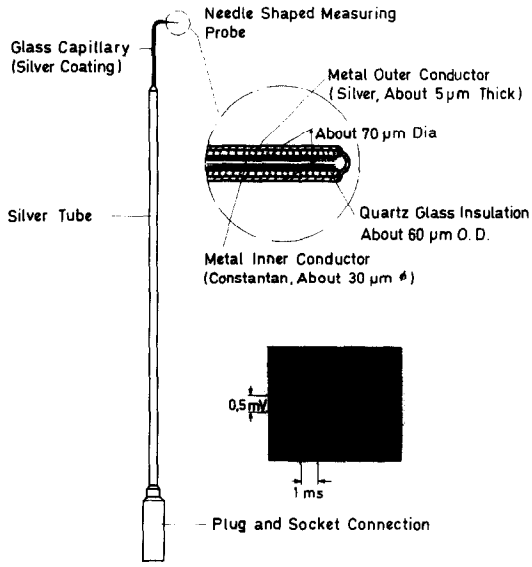

FIG. 1. Thermocouple layout—silver–constantan pair.

It has a measuring junction of about 35 µm at its top. The response time τ is ~0.5 ms if water is dropped onto it. In superheated steam response times of 3–7 ms are measured depending on the operating conditions. The measuring probe penetrates like a needle the interface of the steam bubble during growth at the orifice and rising in water, respectively. When the bubble leaves the probe, it is surrounded by water for some time before the consecutive bubble hits the measuring junction. In this way the temperature difference can be determined between the steam bubbles and the water. Phase change occurs at 20–75 Hz depending on the frequency of bubble formation.

RESULTS OF EXPERIMENTS

The majority of experiments have been performed at system pressures of 40, 80, 120 and 160 at. Three steam superheats (100, 150 and 200 K) have been investigated. The flow rate of superheated steam is varied so that a zone is covered beginning with steady-state single bubble formation in the dynamic range then transition to non-steady-state aeration until bubble chains are formed. The orifice diameter of cylindrical single orifices is varied in three steps, $d = 1.5$ mm, $d = 2$ mm and $d = 3$ mm, while the height of the orifice has a constant value of 4 mm.

At a distance of about 2 mm from the orifice inlet the steam temperature in the antechamber is measured by a sheathed thermocouple of 0.25 mm OD. Related to this measuring point the three superheatings of steam are set at 100, 150 and 200 K. The temperature of live steam T_0 entering the bubble and the temperature of the detaching bubbles, T_{Ab}, are measured with the needle-shaped thermocouple and in most of the experiments the bubble temperatures are measured at a distance of about 5 and 10 mm, in some experiments

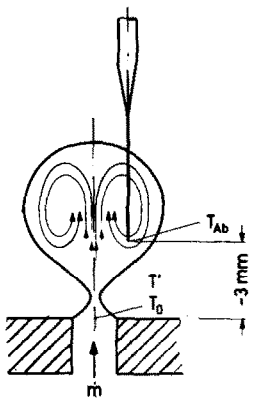

FIG. 2. Temperature measurement of the detaching bubble.

also of about 40 mm from the orifice plate. Figure 2 shows the place of installation of the thermocouple at which the temperature T_{Ab} of the detaching bubble is determined.

The thermocouple is shifted laterally so that the average temperature of the bubble and not the temperature of the entering live steam is measured.

The measuring values are recorded synchronously with film exposure. The position of the measuring place related to the orifice plate can be seen from the films. Depending on the sequence of bubbles, the superheat temperatures of 80–200 different bubbles are measured for each series of experiments and the average superheat temperature is determined from these values.

Figure 3 shows such superheat temperatures plotted versus the mass flow rate through a 3 mm dia. orifice. The steam superheats are related to superheating in the antechamber, i.e. to live steam superheat. The discontinuous plots, these are the three upper plots, show the normalized superheat of steam entering the bubble. The lower plots show the normalized superheat of bubbles at the moment of detachment. The system pressures are the parameters. Considerable cooling of the live steam can be found while it flows through the orifice at low mass flow rates. Nearly independent of the temperature of the steam entering the bubble almost the same degree of heat removal is attained during bubble formation. While in the range of steady-state aeration the temperature is reduced by more than 60% at the time of bubble detachment, less than 40% of the supplied energy is transferred during bubble formation when turbulent aeration has started (definition of ranges cf. Part I).

Figure 4 is a plot of superheat temperatures of bubbles versus the path covered while they ascend through the water. This diagram makes clear the high significance of heat transfer during bubble formation. At the value $h = 3$ mm on the abscissa the temperature of the detaching bubble is marked. If the measuring point lies about 6 mm above the orifice plate, the initial temperature difference has already been reduced to a high degree. The steam flowing into the bubble through the orifice causes a strong inner turbulence of the bubble. This turbulence has been almost eliminated after some 10 mm of bubble ascent path. It is preserved up to this point by strong bubble movement due to the detachment. By reaching a regular steady-state bubble rising a considerable deceleration in temperature reduction can be observed.

EVALUATION

When superheated steam flows into water having the temperature of saturation superheated bubbles are formed. Bubble growth is given by the feed of superheated steam through the orifice. This phase continues until detachment takes place. Due to the temperature gradient existing between the superheated steam and the saturated water, heat is transported to the interface. Since the water is at saturation temperature, it evaporates into the bubble at the phase boundary. The resistance to the heat transfer occurs only in the steam phase.

The calculation of heat-transfer coefficients during

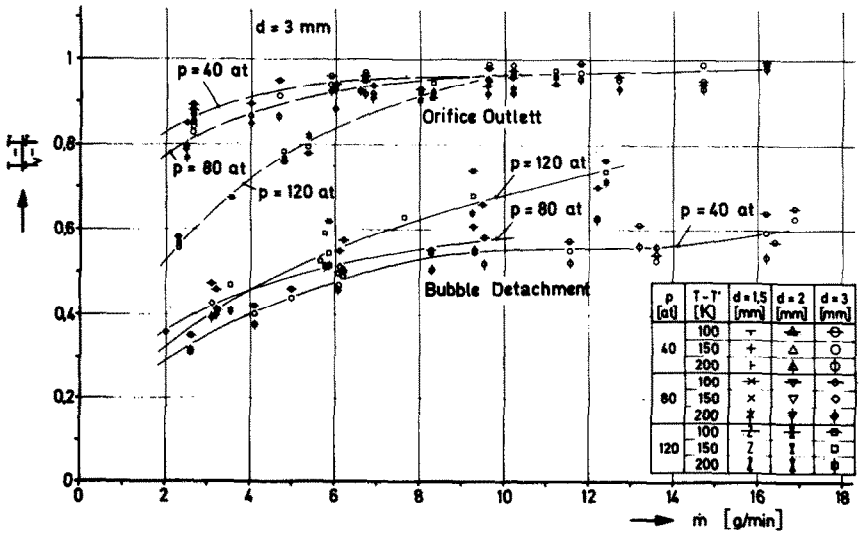

FIG. 3. Dimensionless steam superheat.

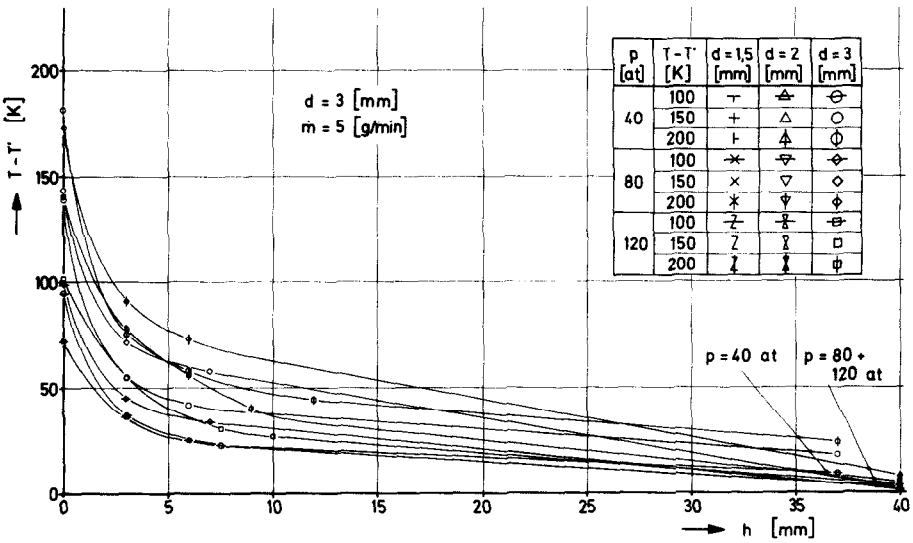

FIG. 4. Bubble temperature during ascent.

bubble formation at orifices is based on the following assumptions:

(1) In the interior of the bubble exists the temperature $T(t)$ spatial constant but variable with time.
(2) The existing temperature gradient between the steam and water is reduced within a boundary layer on the steam side.
(3) The water is at saturation temperature.

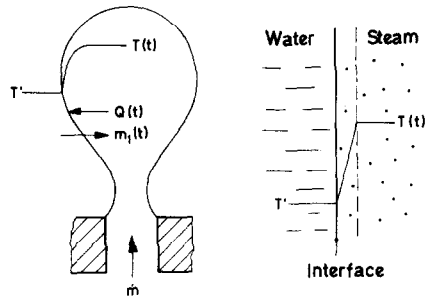

FIG. 5. Temperature development within the bubble (schematic).

The condition that phase transition is an isothermal isobaric process implies that the specific free enthalpy g in both phases takes the same value near the interface.

$$dg' = -s'\,dT + v'\,dp = dg'' = -s''\,dT + v''\,dp. \quad (1)$$

The Clausius–Clapeyron equation follows from relation (1) with $s''-s' = r/T'$:

$$\frac{dp}{dT} = \frac{s''-s'}{v''-v'} = \frac{r}{T'(v''-v')}. \quad (2)$$

According to Laplace the pressure in the bubble is higher than in the surrounding water by the action of surface tension force:

$$\Delta p_1 = \frac{2\sigma}{R}. \quad (3)$$

Furthermore, according to Lord Kelvin, the vapor pressure of the curved surface is smaller than the saturation pressure of the plane surface.

$$\Delta p_2 = \frac{2\sigma}{R}\cdot\frac{P''}{\rho'-\rho''}. \quad (4)$$

The summation of these two partial pressures $\Delta p_1 + \Delta p_2$ yields the necessary augmentation in vapor pressure Δp which is needed for the existence of the bubble:

$$\Delta p = \frac{2\sigma}{R}\cdot\frac{\rho'}{\rho'-\rho''}. \quad (5)$$

Introducing equation (5) in equation (2) yields the temperature augmentation of water which is necessary to enhance the steam pressure:

$$\Delta T = \frac{T'(v''-v')}{r}\cdot\frac{2\sigma}{R}\cdot\frac{\rho'}{\rho'-\rho''}. \quad (6)$$

In these investigations the water superheats required to obtain the equilibrium of phases are in the order of 10^{-4} K.

During aeration through orifices large-volume bubbles are formed for which the influence of boundary surface tensions and boundary surface curvatures is of secondary importance so that the assumptions made under (2) and (3) are admissible.

So, an average heat-transfer coefficient during bubble formation can be formed by equating the heat flux towards the interface with the reduction in steam enthalpy of the supplied live steam into the bubble.

Steam superheating is the cause of heat transfer between the bubble and the surrounding water. Thus, the temperature difference between the steam temperature T and the constant water temperature T' gets steadily smaller during bubble formation (cf. Fig. 4). This leads to the schematic temperature development shown in Fig. 6.

This representation is based on constant surface and massflow rates. With the heat-transfer coefficient α the heat flux to a surface element is obtained.

$$dq = \alpha(T-T')\,dO. \quad (7)$$

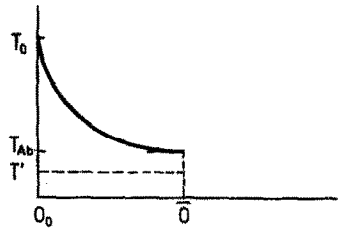

FIG. 6. Temperature curve in a growing bubble.

The change of temperature of the bubble during its formation is given by:

$$dq = -\dot{m}c_p dT. \tag{8}$$

By equating and solving for the temperatures the following expression is obtained with the integration constant $(T_0 - T')$ as the initial temperature difference:

$$(T - T') = (T_0 - T')e^{-(\alpha O/\dot{m}c_p)}. \tag{9}$$

By eliminating q we have the average heat-transfer coefficient during bubble formation at orifices:

$$\alpha = \frac{\dot{m}c_p}{\bar{O}} \ln \frac{T_0 - T'}{T_{Ab} - T'}. \tag{13}$$

The heat-transfer coefficient indicated in equation (13) contains a bubble surface $\bar{O}$ averaged over the time of formation and the logarithm of the quotient of the temperature gradient between the steam and the water at the beginning and at the end of bubble formation. It must be considered as a coefficient for the heat flux from the bubble to the interface. This heat flux causes the water to evaporate into the bubble and the steam to rise to the level of temperature corresponding to the bubble.

The coefficient of transfer so defined has been plotted in Fig. 7 vs the Reynolds number.

The physical properties of the *Re*-number are related

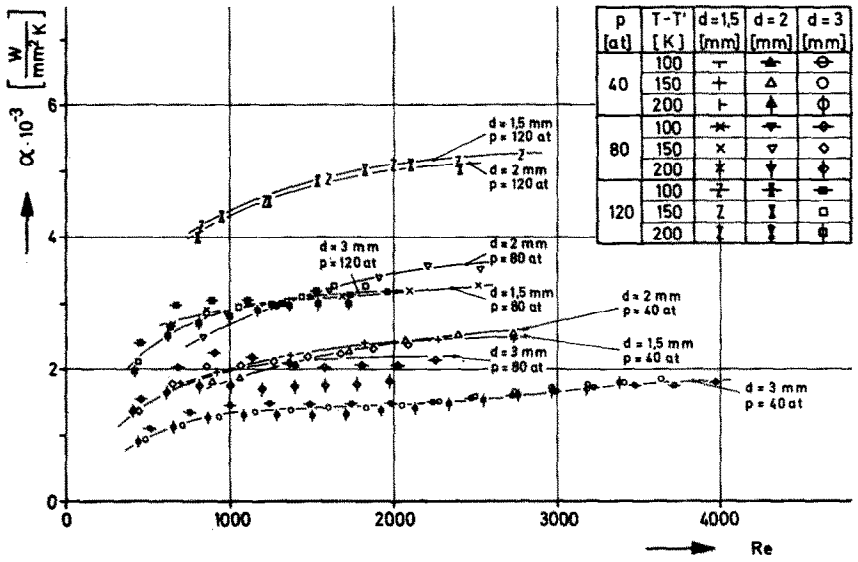

FIG. 7. Heat-transfer coefficient.

This yields for the temperature difference during bubble formation:

$$(T_{Ab} - T') = (T_0 - T')e^{-(\alpha \bar{O}/\dot{m}c_p)}. \tag{9a}$$

After introduction of equation (9) in (7) and integration over the surface we obtain:

$$q = \dot{m}c_p[(T_0 - T') - (T_{Ab} - T')]. \tag{10}$$

After transformation of (9a) into

$$\frac{\alpha \bar{O}}{\dot{m}c_p} = \ln \frac{T_0 - T'}{T_{Ab} - T'}$$

and introduction of this expression into equation (10) the heat flux becomes:

$$q = \alpha \bar{O} \frac{(T_0 - T') - (T_{Ab} - T')}{\ln \dfrac{T_0 - T'}{T_{Ab} - T'}}. \tag{11}$$

The reduction in enthalpy of the live steam flow supplied to the bubble is

$$q = \dot{m}c_p(T_0 - T_{Ab}). \tag{12}$$

to the system pressure and the steam temperature at the orifice outlet. The orifice diameter has been introduced as the characteristic length. Parameters are the orifice diameter and the system pressure.

An increase in the system pressure from 40 to 120 at results in higher heat-transfer coefficients, which can be explained in the following way:

The heat of evaporation decreases with increasing system pressure. Less energy must be supplied to the water to allow its change into the vapor phase. So, more water can be evaporated for a given heat resistance and time interval. At the same time, the kinematic viscosity ν decreases. This reduces the thickness of the boundary layer which represents the barrier for the heat transfer. Since the heat conduction λ increases with the pressure, this leads to an increase in the heat-transfer coefficients; the evaporated water gains faster the average bubble temperature.

On the other hand, a change in the superheat temperature of the live steam has no significant influence on the heat transfer at constant system pressure.

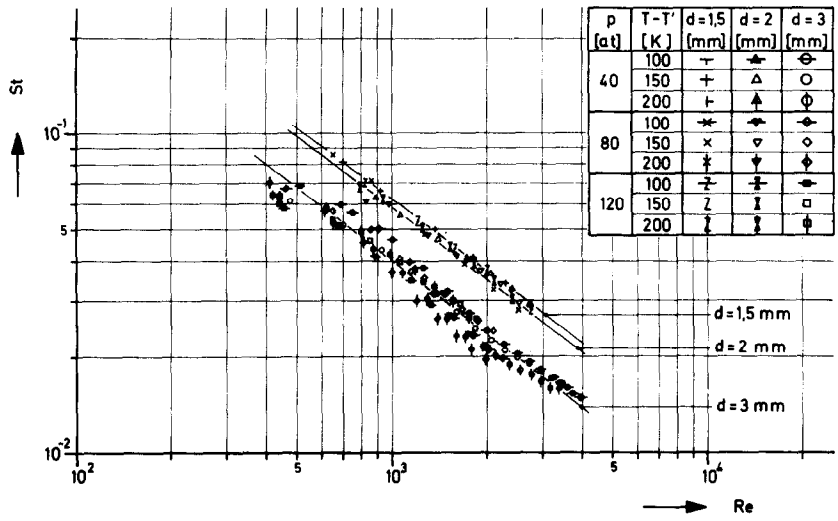

FIG. 8. Dimensionless heat-transfer coefficient.

With increasing steam temperature both the heat conduction and the viscosity increase. Higher viscosity, however, leads to a growth in the thickness of the boundary layer so that the influence of the improved heat conduction is eliminated. The heat-transfer coefficients increase with the mass flow rate through the orifice. At $Re \approx 1300$ the transition from steady-state to non-steady-state aeration is observed at the system pressures under consideration. In the non-steady-state range the coefficient of transfer grows but very slowly which leads to the conclusion that the turbulence within the bubbles cannot be substantially enhanced.

Furthermore, the tendency can be observed that smaller orifices with small bubble volumes generated in short periods of formation are marked by higher heat-transfer coefficients.

By considerations based on mechanics of similarity a generalization of the experimental results is attempted. As a result of dimensional analysis a dimension matrix is obtained which yields non-dimensionalized characteristics.

By appropriate combination of these characteristics the Stanton number is obtained which allows uniform representation of measuring results.

In Fig. 8 the Stanton number has been plotted vs the Reynolds number for orifices of 1.5, 2, 3 mm dia. The Stanton number has been established according to the following relation:

$$St = \frac{Nu}{Pe} = \frac{\alpha bd}{\dot{m}c_p}. \tag{14}$$

Accordingly, the heat-transfer coefficient is represented as the ratio of the Nusselt number to the Péclet number and thus as the ratio of the heat flux due to heat transfer to the enthalpy flow rate related to mass. The decrease in the Stanton number with increasing *Re*-number implies that the greater enthalpy flow rate supplied which is associated with an increase in mass flow rate cannot be reduced by greater heat transfer. Consequently, the temperature of bubble detachment increases with the flow rate through the orifice. While the data of the 1.5 mm dia. orifice are slightly higher than the data of the 2 mm dia. orifice, the distance from the 3 mm dia. orifice becomes quite substantial; the Stanton numbers are lower by about 30%. For small orifices small bubbles are observed at the same mass flow rate, which are characterized by a higher frequency of formation than at large orifices. The bubbles grow faster which causes an improvement of heat transfer.

The following relation obtained from the representation of results is derived for the heat-transfer coefficient α:

$$\alpha = B\frac{\dot{m}c_p}{bd} Re^M. \tag{15}$$

With the values for the exponent $M = -0.766$ and for the ordinate sections B

d(mm)	B
1.5	12
2	11
3	8

Using these values the heat-transfer coefficients measured in the pressure and temperature ranges under consideration can be reproduced within deviations of 15% for some measurements within 20%.

To obtain these results the following parameters are varied.

Orifice diameter: $d = 1.5; 2; 3$ (mm), cylindrical

Mass flow rate: $\dot{m} = 2$ to 20 (g/min)

System pressure: $p = 40; 80; 120$ (at)

Superheat temperature: $T_V - T' = 100; 150; 200$ (K).

The following is a summary of experimental datas performed with the 3 mm dia. orifice in other ranges of system pressures. The measured results of these experiments are compared with the values obtained by introduction of the respective measured values in the formulae derived in the parameter study.

p (at)	$\dot{m}$ (g/min)	α $\left(\frac{W}{cm^2 K}\right)$	α_R $\left(\frac{W}{cm^2 K}\right)$	$\Delta\alpha$ (%)
15.1	1.10	0.0526	0.0659	−25.3
149	4.98	0.364	0.409	−11
160.2	1.765	0.748	0.442	41
159.5	1.765	0.403	0.336	9.1
161	5.27	0.548	0.461	15.8

The results allowing indications on the heat-transfer coefficients show that an extrapolation to higher system pressures seems to be justified. Also for system pressures $p < 40$ at the expression indicated seems to be applicable to the transfer coefficient.

SUMMARY

The results first obtained in this study for the heat-transfer coefficient between superheated steam and saturated water during bubble formation at the orifices with high system pressures range from $\alpha = 0.05$ to $0.75(W/cm^2 K)$. The heat-transfer coefficients must be regarded as proportionality factors for the heat flux which causes the evaporation of water at the bubble boundary and heating up of the evaporated water to the average bubble temperature. A useful dimensionless characteristic is the Stanton number which represents the ratio of the transferred amount of heat to the enthalpy flow due to forced convection. The heat-transfer coefficients grow with increasing system pressure, with decreasing orifice diameter and to a less extent with the superheated steam mass flow rate. Thus, the following attributions can be made: high transfer coefficients for small orifices and high system pressures, respectively, low transfer coefficients for large orifices and low system pressures, respectively.

Grassmann and Wyss [3] propose integral heat-transfer coefficients for water and steam at atmospheric pressure, i.e. values averaged over bubble formation and ascent. At a maximum temperature difference of 80 K between superheated steam and saturated water α-values between 0.02 and $0.05(W/cm^2 K)$ are measured. The orifice diameter is 1.2 mm in this case.

In this paper the minimum numerical value was determined for the transfer coefficient $\alpha = 0.05(W/cm^2 K)$ at a large orifice ($d = 3$ mm) and low system pressure ($p = 15$ at). Comparing these influences which are caused by different orifice diameters, system pressures, and measuring methods, a connection between the two different measurements seems to be possible.

For slightly superheated and subcooled water and saturated steam, respectively, Grassmann and Wyss [3] determined transition coefficients between $\alpha = 7.5$ and $11.5(W/cm^2 K)$, respectively.

At high system pressures heat-transfer coefficients of $0.75(W/cm^2 K)$ on the steam side were measured in this work.

A comparison shows that despite the considerable increase in heat transfer with increasing system pressure and heat resistance on the steam side the transfer of heat is better by roughly one order of magnitude in case of heat resistance on the water side.

Acknowledgement—The author wishes to thank Prof. U. Müller for the great interest and promotion of this work. He is grateful to Dr. J. Reimann for many discussions and to Mr. E. Eggert for assistance in carrying out the experiments.

REFERENCES

1. P. Grassmann, *Physikalische Grundlagen der Verfahrenstechnik*, 2. Auflage. Sauerländer, Aarau und Frankfurt a.M. (1967).
2. M. R. L'Ecuyer, An investigation of the energy transfer from a liquid to a gas bubbling through the liquid, Ph.D. Thesis, Purdue University, Ann Arbor, Michigan (August 1964).
3. P. Grassmann and E. Wyss, Bestimmung von Wärme- und Stoffübergangszahlen zwischen Dampfblase und Flüssigkeit, *Chemie-Ingr-Tech.* **34**(11), 755–759 (1962).
4. H. Schmidt, Schnelle, koaxiale Mini-Thermoelemente, *Arch. Tech. Messen* **3**, 53–56 (1973).

FORMATION DES BULLES ET TRANSFERT THERMIQUE PENDANT LA DISPERSION DE LA VAPEUR SURCHAUFFEE DANS L'EAU SATURANTE. 2EME PARTIE: TRANSFERT THERMIQUE ENTRE LES BULLES DE VAPEUR SURCHAUFFEE ET L'EAU SATURANTE DURANT LA FORMATION DE LA BULLE

Résumé—Dans les évaporateurs, caractérisés par l'introduction de la vapeur surchauffée dans l'eau à évaporer, la vapeur est distribuée par une plaque perforée. La vapeur est introduite dans l'eau à travers une multitude de trous cylindriques. En vue de la construction optimale de tels évaporateurs le parcours minimal de transfert thermique pendant lequel la bulle perd sa surchauffe est très important. Le transport d'énergie pendant la formation de la bulle peut devenir significatif dans le transport total d'énergie. La première partie du rapport concernait la formation des bulles de vapeur, leur taille, leur forme et leur fréquence pour des pressions et des températures élevées. Cette partie du travail décrit le transfert thermique durant le formation des bulles. Dans le domaine de pression considéré entre 15 et 160 bar on mesure une décroissance de la température de surchauffe de 40–60% pendant la formation de la bulle. Les coefficients moyens de transfert varient entre 0,05 et 0,75 $W/cm^2 K$. Le transfert thermique est exprimé par le nombre de Stanton qui est fonction du nombre de Reynolds.

BLASENBILDUNG UND WÄRMEÜBERTRAGUNG BEIM EINBRINGEN VON HEISSDAMPF IN WASSER VON SÄTTIGUNGSTEMPERATUR—II WÄRMEÜBERTRAGUNG VON HEISSDAMPFBLASEN AN GESÄTTIGTES WASSER WÄHREND DER BLASENBILDUNG

Zusammenfassung—Bei Mischverdampfern, die gekennzeichnet sind durch das Einführen von überhitztem Dampf in zu verdampfendes Wasser, erfolgt die Dampfverteilung über sog. Siebböden. Durch eine Vielzahl zylindrischer Bohrungen wird der Dampf in das Wasser eingebracht. Für die optimale Auslegung solcher Verdampfer ist die minimale Strecke der Wärmeübertragung von Interesse, die die Heissdampfblasen bis zu ihrer Enthitzung zurücklegen. Dabei kann der Energietransport während der Blasenbildung wegen seiner Grösse signifikant für den Gesamttransport werden.

Im Teil 1 wurde über die Bildung von Heissdampfblasen, deren Grösse, Form und Bildungsfrequenz bei hohen Systemdrücken und Systemtemperaturen berichtet.

Gegenstand des vorliegenden Teils 2 ist die Angabe der Wärmeübertragung während der Periode der Blasenbildung.

In dem experimentell betrachteten Systemdruckbereich von $p = 15$–160 at wird während der Blasenbildung eine Abnahme der Überhitzungstemperatur von 40 bis 60% gemessen. Die mittleren Wärmeübergangszahlen liegen dabei zwischen 0,05 und 0,75 W/cm² K. Die Wärmeübertragung wird durch eine Beziehung Stantonzahl als Funktion der Reynoldszahl angegeben.

ОБРАЗОВАНИЕ ПУЗЫРЬКОВ И ПРОЦЕСС ПЕРЕНОСА ТЕПЛА ПРИ ДИСПЕРСИИ ПЕРЕГРЕТОГО ПАРА В НАСЫЩЕННОЙ ВОДЕ. ЧАСТЬ 2. ПЕРЕНОС ТЕПЛА ОТ ОБРАЗУЮЩИХСЯ ПУЗЫРЬКОВ ПЕРЕГРЕТОГО ПАРА К НАСЫЩЕННОЙ ВОДЕ

Аннотация — В выпарных аппаратах, принцип работы которых основан на вводе перегретого пара в испаряемую воду, пар распределяется по так называемым сопловым сегментам и подается через множество цилиндрических отверстий. Для расчета оптимальной конструкции таких аппаратов необходимо определить минимальную длину участка, на котором происходит отдача пузырьками теплоты перегрева. Что касается величины теплового потока, то существенное влияние на нее может оказывать перенос тепла в момент зарождения пузырьков. В первой части работы рассматривались образование пузырьков перегретого пара, их диаметр, форма и частота образования при высоком давлении и температуре в системе. В данной части описывается процесс переноса тепла в период образования пузырьков. В исследуемом диапазоне давлений в системе от 15 до 160 атм температура перегрева во время образования пузырьков снижалась от 40 до 60%. Средние коэффициенты теплообмена изменялись от 0,05 до 0,75 вт/см² К. Процесс переноса тепла описывается числом Стантона в функции числа Рейнольдса.